Mode Analysis and Stabilization of a Spatial Power Combining Array with Strongly Coupled Oscillators

Shigeji Nogi, *Member, IEEE,* Jenshan Lin, *Student Member, IEEE,* and Tatsuo Itoh, *Fellow, IEEE*

***Abstract*—In order to attain stabilized power-combining operations of a strongly coupled active antenna array, mode analysis for the multi-moding problem of the array is presented, and an effective method for exciting only the in-phase power-combining mode is proposed. In a one-dimensional array of active antennas coupled mutually through microstrip lines, the frequencies and the voltage distributions of the normal modes are obtained. Stable modes of the array are identified using the averaged potential theory. Time evolutions of the mode amplitudes are also calculated. In order for only the desired power-combining mode to oscillate, appropriate resistors are introduced at the midpoints of the coupling lines between the active antennas. An experiment for the arrays with up to eight active antennas has been carried out using Gunn diodes. It has been confirmed that the introduction of the resistors is effective for stable excitation of the in-phase power-combining mode.**

I. Introduction

In order to obtain solid-state high power sources at the millimeter region, power combining of a large number of active devices is inevitable since available power of a single solid-state device decreases remarkably with an increasing frequency [1]. Recently, the quasi-optical approach to power combining has been proposed to be the most promising technique at this frequency region. So far, two types of approach have been reported. One constitutes an oscillator with a Fabry–Perot resonator which contains a grid [2], [3] or a grating [4] mounted with many active devices, while another forms an array of active antennas accompanied with coupled oscillators [5]–[9].

In the active antenna array, many individual oscillators are synchronized through mutual coupling [5]–[7], or by an external signal injection [8], [9]. The mutual coupling type has an advantage over the external signal injection type in the simplicity of circuit configuration. In the active antenna array with a very large number of mutually coupled oscillators, however, there are usually several modes which can be excited, and the oscillation in the power-combining mode is not necessarily ensured [10]; this is so-called the multi-moding problem. Therefore, it is important for stable power combining to overcome the multi-moding problem by letting only the desired power-combining mode to oscillate.

Manuscript received August 13, 1992; revised March 11, 1992.

The authors are with the Department of Electrical Engineering, University of California, Los Angeles, Los Angeles, CA 90024-1594. S. Nogi is on leave from the Department of Electrical and Electronic Engineering, Okayama University, Okayama 700, Japan.

IEEE Log Number 9211940.

The multi-moding problem has been discussed not only in the oscillators with multiple-device cavities [11], [12] but also in the active antenna arrays [5], [6], [13]. However, for arrays with a large number of active antenna elements, it seems that neither an explicit analytical expression of the condition for stable oscillations nor an effective technique to stabilize the desired mode of oscillation has been given yet.

In this paper, we consider the multi-moding problem in a one-dimensional array of active microstrip antennas with strongly coupled oscillators. We take a mode analysis approach which is capable of treating arrays with a number of active antennas on the assumption of identical characteristics of the array elements, and propose a method for overcoming this problem. In Section II, we obtain the frequencies and the voltage distributions of the normal modes of this array. In Section III, criteria for stability of the modes are clarified using the averaged potential theory [14] which gives a powerful method for analyzing multi-mode oscillators. The stable modes of the system are obtained by the use of the criteria. Time evolutions of the mode amplitudes from the initial states caused by noise to the settled states are also calculated. Section IV is devoted to show that introduction of appropriate resistors into the coupling lines between the oscillators can suppress all the undesired modes and ensure the oscillation in the power-combining mode. In Section V, we carry out an experiment using Gunn diodes and compare the experimental result with the theoretical one.

II. Normal Modes in a One-Dimensional Array of Coupled Oscillators

A. Structure and Equivalent Circuit

The configuration of a one-dimensional array of N coupled oscillators is shown in Fig. 1. Each oscillator, consisting of a patch antenna and a two-terminal active device, loads periodically a microstrip transmission line at an interval of d. Fig. 2 shows the equivalent circuit of the array. Each two-terminal active device is denoted by a negative conductance, while the patch antenna portion looking from the device is represented by the parallel combination of the capacitance C, the inductance L and the load conductance G_L. The current in the negative conductance of the device is J_k $(k = 1, 2, \cdots, N)$ Any reactive element in the active device may be absorbed into the passive L and C for the purpose of the analysis.

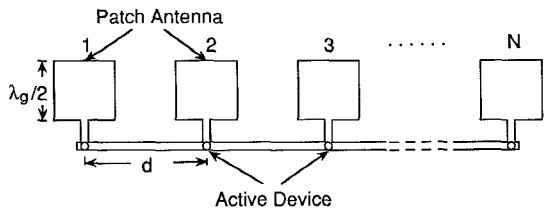

Fig. 1. One-dimensional array of N coupled oscillators.

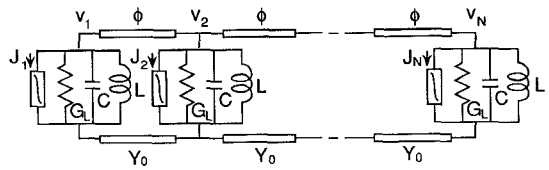

Fig. 2. Equivalent circuit representation for the array.

The microstrip coupling line has a characteristic admittance Y_0. The electrical length between adjacent devices is $\phi = \beta(\omega)d$, where $\beta(\omega)$ is the phase constant at an angular frequency ω. Since no dispersion is assumed, for simplicity, β is proportional to ω in the following analysis.

B. Normal Modes

If each resonant path antenna structure has a high Q-factor, the frequencies and the voltage distributions of normal modes of the array can be approximately determined by the reactive system which is obtained by removing all of the negative and the load conductances from the circuit in Fig. 2. Let us represent the voltage at the node of the kth LC-resonant circuit as $v_k = R_e\left(V_k e^{j\omega t}\right)$ in the reactive system. Here, v_k is the time domain instantaneous voltage, and V_k is a phaser but is real, because the system is now reactive. For the reactive system, the circuit equations are

$$\begin{aligned} j(b+b_d)V_1 + jb_tV_2 &= 0 \\ jb_tV_{k-1} + j(b+2b_d)V_k + jb_tV_{k+1} &= 0 \\ k &= 2,3,\cdots,N-1 \\ jb_tV_{N-1} + j(b+b_d)V_N &= 0 \end{aligned} \tag{1}$$

where

$$b = (\omega C - 1/\omega L)/Y_0 = Q_{ex}(\Omega - 1/\Omega) \tag{2a}$$
$$b_d = -\cot\phi = -\cot(\phi_0\Omega) \tag{2b}$$
$$b_t = \operatorname{cosec}\phi = \operatorname{cosec}(\phi_0\Omega) \tag{2c}$$

with

$$\omega_0 = 1/\sqrt{LC} \tag{2d}$$
$$\Omega = \omega/\omega_0 \tag{2e}$$
$$\phi_0 = \beta(\omega_0)d \tag{2f}$$
$$Q_{ex} = \omega_0 C/Y_0\,. \tag{2g}$$

ϕ_0 is the electrical length of each coupling line at the resonant frequency ω_0 of each patch antenna, and then $\phi_0\Omega$ is the electrical length of this line at the frequency ω. Equation (1) is written in the vector equation as

$$jb\begin{bmatrix} V_1 \\ V_2 \\ \cdot \\ \cdot \\ \cdot \\ V_N \end{bmatrix} + jb_t\boldsymbol{B}\begin{bmatrix} V_1 \\ V_2 \\ \cdot \\ \cdot \\ \cdot \\ V_N \end{bmatrix} = 0 \tag{3}$$

where

$$\boldsymbol{B} = \begin{bmatrix} \gamma & 1 & & & & 0 & \\ 1 & 2\gamma & 1 & & & & \\ & 1 & 2\gamma & \cdot & & & \\ & & \cdot & \cdot & \cdot & & \\ & & & \cdot & \cdot & \cdot & \\ & & & & \cdot & \cdot & \cdot \\ & 0 & & & 1 & 2\gamma & 1 \\ & & & & & 1 & \gamma \end{bmatrix} \tag{4a}$$

with

$$\gamma = b_d/b_t = -\cos(\phi_0\Omega)\,. \tag{4b}$$

In the left hand side of (3), the first and second term correspond respectively to the currents flowing through the LC resonant circuits and to the currents toward the coupling lines at each node.

Let us denote the ith eigenvalue and the corresponding eigenvector of the matrix $\boldsymbol{B}$ as λ_i and $\boldsymbol{p}_i = [p_{1i}, p_{2i}, \cdots, p_{Ni}]^t$, respectively. The ith eigenvalue of the matrix $jb_t\boldsymbol{B}$, $jb_t\lambda_i$, gives the common admittance looking toward the coupling lines at each LC-resonant circuit when the voltage at the kth LC-resonant circuit takes the distribution of the ith mode, $V_k^{(i)} = Ap_{ki}$ $(k = 1,2,\cdots,N)$, with an arbitrary constant A. Equation (3) shows that since the admittance of each LC-resonant circuit is jb, the frequency Ω_i of the ith normal mode of the reactive system can be given by

$$b + b_t\lambda_i = 0\,. \tag{5}$$

The ith eigenvalue λ_i of the matrix $\boldsymbol{B}$ is obtained as

$$\lambda_i = 2(\cos\xi_i + \gamma)\,. \tag{6a}$$

Here, γ takes a discrete value γ_i as

$$-\gamma_i = \cos(\phi_0\Omega_i) = \begin{cases} \dfrac{\cos\left(\frac{N+1}{2}\xi_i\right)}{\cos\left(\frac{N-1}{2}\xi_i\right)}: & \text{cos-modes} \\ \dfrac{\sin\left(\frac{N+1}{2}\xi_i\right)}{\sin\left(\frac{N-1}{2}\xi_i\right)}: & \text{sin-modes} \end{cases} \tag{6b}$$

(See Appendix I). Two-types of solutions in (6b) are named as 'cos-modes' and 'sin-modes' due to the voltage distributions. The corresponding eigenvector $\boldsymbol{p}_i = [p_{1i}, p_{2i}, \cdots, p_{Ni}]^t$ is given by

$$p_{ki} = \begin{cases} \sqrt{\dfrac{2\sin\xi_i}{N\sin\xi_i + \sin(N\xi_i)}}\cos\left\{\left(k - \frac{N+1}{2}\right)\xi_i\right\}, \\ \text{for cos-modes} \\ \sqrt{\dfrac{2\sin\xi_i}{N\sin\xi_i - \sin(N\xi_i)}}\sin\left\{\left(k - \frac{N+1}{2}\right)\xi_i\right\}, \\ \text{for sin-modes} \end{cases}$$
$$k = 1,2,\cdots,N \tag{7}$$

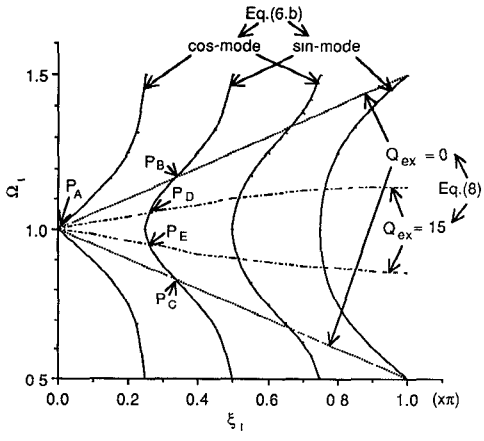

Fig. 3. Graphical representation of (5b) and (8) for the case of $N = 4$ and $\phi_0 = 2\pi$.

where $\sum_{k=1}^{N} p_{ki}^2 = 1$ is imposed for normalization.

Substituting (2a), (2c), (4b) and (6a) into (5) yields

$$-\frac{1}{2} Q_{\mathrm{ex}} \left(\Omega_i - \frac{1}{\Omega_i} \right) \sin(\phi_0 \Omega_i) + \cos(\phi_0 \Omega_i) = \cos \xi_i \,. \quad (8)$$

Solving the simultaneous equation (8) and (6b) numerically gives the values of Ω_i and ξ_i.

In the following, we consider the case of $\phi_0 = 2\pi$ and $0.5 \leq \Omega \leq 1.5$. Fig. 3 gives graphical representation of (8) and (6b) for $N = 4$. The intersections of two curves, such as P_A and P_B, correspond to Ω_i's and ξ_i's. There exist $(2N-1)$ modes in this frequency range $(0.5 \leq \Omega \leq 1.5)$.

When $Q_{\mathrm{ex}} = 0$, as the susceptances of the LC resonant circuits looking from the coupling lines vanish, the normal modes are reduced to the standing wave modes on an open-ended transmission line of a length of $(N-1)$ wavelengths at $\omega = \omega_0$. The solution for this case given from (6b) and (8) by $\xi_i = (i-1)\pi/(N-1)$ and $\Omega_i = 1 \pm (i-1)/\{2(N-1)\}$, $i = 1, 2, \cdots, N$ corresponds to the standing wave mode which has $\{N - 1 \pm (i-1)/2\}$ wavelengths on the line. In Fig. 3, for instance, the length of the transmission line is three times the wavelength at $\omega = \omega_0$, and the points P_A $(i = 1), P_B$ $(i = 2$, the upper sign) and P_C $(i = 2$, the lower sign) correspond to the modes with three, three and a half, and two and a half wavelengths on the line, respectively.

On the other hand, as Q_{ex} increases, the frequency spacings between adjacent modes for a given i become narrower because of frequency dependence of susceptances of the LC resonant circuits (See P_B and P_C are changed to P_D and P_E, respectively). When $Q_{\mathrm{ex}} > 10$, the solutions can be well approximated by

$$\xi_i \cong \frac{\pi}{N} \left\{ i - 1 + \frac{1}{Q_{\mathrm{ex}}} \sin \frac{(i-1)\pi}{N} \right\} \quad (9a)$$

$$\Omega_i \cong 1 \pm \frac{1}{\sqrt{\pi Q_{\mathrm{ex}}}} \sin \frac{(i-1)\pi}{2N} + \frac{1}{4\pi Q_{\mathrm{ex}}} \sin^2 \frac{(i-1)\pi}{2N} \quad i = 1, 2, \cdots, N \,. \quad (9b)$$

Because there are two (ξ_i, Ω_i) values with very close values for $i \neq 1$, we number each mode in increasing values of ξ_i as

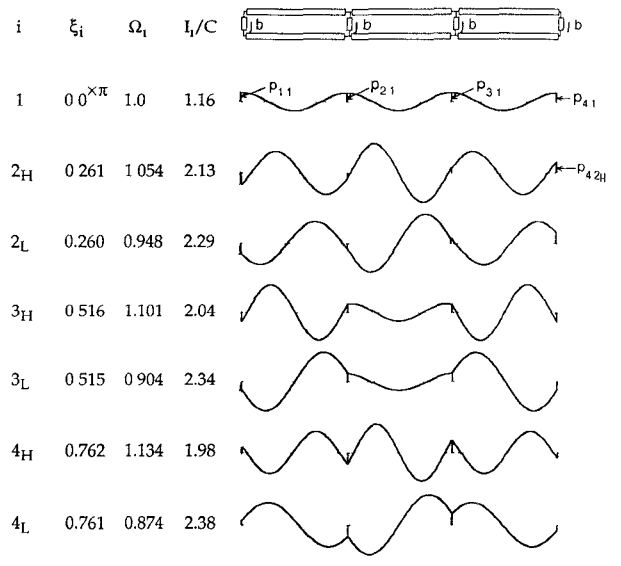

Fig. 4. Modes for the case of $N = 4$ ($\phi_0 = 2\pi$, $Q_{\mathrm{ex}} = 15$).

$1, 2, \cdots$ with subscript H for $\Omega_i > 1$ and L for $\Omega_i < 1$. For instance, in Fig. 3, the points P_D and P_E correspond to the mode 2_H and 2_L, respectively, for the case of $Q_{\mathrm{ex}} = 15$. In this paper, we write the subscript H or L only when distinction is needed. In contrast, $i + 1$ gives the single value of $\xi_1 = 0$ and $\Omega_1 = 1$ which corresponds to the point P_A in Fig. 3; for this special case, (7) is reduced to

$$p_{k1} = \frac{1}{\sqrt{N}} \qquad k = 1, 2, \cdots, N \,. \quad (10)$$

Fig. 4 shows not only the frequency and ξ_i value but also the standing wave pattern of each mode on the coupling lines for the case of $N = 4$ and $Q_{\mathrm{ex}} = 15$. Mode $i = 1$ is the desired mode for spatial power combining because all of the antenna elements can oscillate not only in phase but also in equal amplitudes. All other modes are undesirable modes.

III. Analysis of Stable Modes

In this section, we intend to obtain criteria for stability of the mode and to find stable modes in the system.

A. Averaged Potential

We assume the current-voltage characteristic of the active device in Fig. 2 as

$$J_k = -G_1 v_k + G_3 v_k^3, \qquad k = 1, 2, \cdots, N \quad (11)$$

where v_k^2-term is omitted since it has no effect on the analytical result. According to the averaged potential theory [14], such a system as the coupled oscillators in Fig. 2 evolves with time toward the direction in which the averaged potential of the system decreases, and the stable steady-states correspond to the minimum points of this potential (See Appendix II). The averaged potential U for the circuit system in Fig. 2 is given by the time average of the sum of the following quantities for

all the conductances in the system:

$$U = \frac{1}{T} \int_{t}^{t+T} \sum_{k=1}^{N} (Q_{k,a} + Q_{k,L})\, dt \tag{12a}$$

where

$$Q_{k,a} = \int^{v_k} J_k dv_k = -\frac{1}{2} G_1 v_k^2 + \frac{1}{4} G_3 v_k^4, \quad \text{for the } k\text{th device} \tag{12b}$$

$$Q_{k,L} = \int^{v_k} G_L v_k dv_k = \frac{1}{2} G_L v_k^2, \qquad \text{for the } k\text{th load} \tag{12c}$$

Here, a and L in the subscripts denote the active device and the load, respectively. It is assumed that T is sufficiently large so that the integral can be taken over many cycles.

Representing the averaged potential using the normal modes, we can find the behaviors of the normal modes. For this purpose, we have normal mode expansion of v_k as

$$v_k = \sum_i p_{ki} A_i \cos(\Omega_i \omega_0 t + \psi_i) \qquad k = 1, 2, \cdots, N \tag{13}$$

where A_i and ψ_i are the amplitude and the phase of the ith mode, respectively. The summation may be taken over the modes included in the working frequency range of active devices. Using (12b) and (12c) and (13) in (12a) yields

$$U = \frac{1}{4} \left(-\sum_i \alpha_i A_i^2 + \frac{1}{2} \sum_i \sum_j \theta_{ij} A_i^2 A_j^2 \right) \tag{14}$$

where

$$\alpha_i = G_1 - G_L \tag{15a}$$

$$\theta_{ij} = \begin{cases} G_3 \sum_{k=1}^{N} p_{ki}^4, & \text{for } i = j \\ 2G_3 \sum_{k=1}^{N} p_{ki}^2 p_{kj}^2, & \text{for } i \neq j \end{cases} \tag{15b}$$

α_i and θ_{ii} are called the small signal gain parameter and the self-saturation parameter of the ith mode, respectively, and θ_{ij} $(i \neq j)$ is called the mutual-saturation parameter between the ith and jth mode.

Table I gives the matrix $[\theta_{ij}]$ for the same parameters as those used in Fig. 4 ($N = 4$, $\phi_0 = 2\pi$ and $Q_{\text{ex}} = 15$). When Q_{ex} is high, (15b) together with (7) and (9a) gives a rough approximation of θ_{ij} as

$$\frac{\theta_{ii}}{G_3} \cong \begin{cases} 1/N, & \text{for } i = 1,\ 1 + N/2 \text{ (only for even } N) \\ 3/(2N), & \text{otherwise} \end{cases} \tag{16a}$$

and for $i \neq j$

$$\frac{\theta_{ij}}{G_3} \cong \begin{cases} 1/N, & \text{for } i + j = N + 2\ (i, j \neq 1), \text{ and } i = m_H, j = n_L\ (m \neq n) \text{ or } v.v. \\ 3/N, & \text{for } i = m_H,\ j = m_L\ (m \neq i + N/2) \text{ or } v.v. \\ 2/N, & \text{otherwise}. \end{cases} \tag{16b}$$

TABLE I
$[\theta_{ij}]$ FOR THE CASE OF $N = 4$ ($\phi_0 = 2\pi$, $Q_{\text{ex}} = 15$).

$$\frac{1}{G_3}[\theta_{ij}] = \begin{array}{c} \\ 1 \\ 2_H \\ 2_L \\ 3_H \\ 3_L \\ 4_H \\ 4_L \end{array} \begin{array}{c} \begin{array}{ccccccc} 1 & 2_H & 2_L & 3_H & 3_L & 4_H & 4_L \end{array} \\ \begin{bmatrix} .250 & .500 & .500 & .500 & .500 & .500 & .500 \\ .500 & .371 & .743 & .534 & .531 & .277 & .274 \\ .500 & .743 & .372 & .534 & .531 & .277 & .274 \\ .500 & .534 & .534 & .252 & .504 & .469 & .469 \\ .500 & .531 & .531 & .504 & .252 & .472 & .471 \\ .500 & .277 & .277 & .469 & .472 & .353 & .708 \\ .500 & .274 & .274 & .469 & .471 & .708 & .355 \end{bmatrix} \end{array}$$

*We can find from the table that the mode $i = 1$ is stable since $\theta_{11} = 0.25G_3$ and $\theta_{1n} = 0.50G_3$ $(n = 2_H, 2_L, \cdots, 4_L)$ satisfy (22).

B. Steady States and Stability

Now, since we have the averaged potential of the system, we can discuss the steady states of single-mode and simultaneous multi-mode oscillations and their stabilities.

In the case when a single mode, say the ith mode, is excited, the steady-state amplitude of A_i, A_{i0}, is given by the condition $\partial U/\partial A_i|_{A_i = A_{i0}, A_{j(\neq i)} = 0} = 0$ (See Fig. 5(a)). This results in

$$A_{i0}^2 = \alpha_i / \theta_{ii}\,. \tag{17}$$

For the desired power combining mode $i = 1$, as the voltage amplitude at the kth node is expressed as $p_{k1}A_{10}$, the output power supplied to the kth load conductance is given by

$$P_{\text{out},k} = \frac{1}{2} G_L (p_{k1} A_{10})^2\,. \tag{18}$$

Using (10), (15) and (17) in (18) gives

$$P_{\text{out},k} = \frac{G_L(G_1 - G_L)}{2G_3}\,, \tag{19}$$

which takes the maximum value $P_{\text{out},k}^{\max} = G_1^2/(8G_3)$ if the load conductance is chosen as

$$G_L = G_1/2\,. \tag{20}$$

Stability condition can be given by the minimum of the averaged potential. Since U is expressed as the quadratic equation of squares of the mode amplitudes as shown in (14), then (17) gives the minimum point of U with respect to A_i^2. Therefore, the condition for stable single-mode excitation of the ith mode is expressed as

$$\left.\frac{\partial U}{\partial A_n^2}\right|_{A_i = A_{10}, A_{j(\neq i)} = 0} = \frac{1}{4}(-\alpha_i + \theta_{ni} A_{i0}^2) > 0 \quad \text{for all } n\ (\neq i)\,. \tag{21}$$

(See Fig. 5(a)). Because the amplitude of every mode varies toward the direction of decreasing U, (21) means that the mode amplitudes other than the ith mode must decrease near this state even if some noise generates these modes with small amplitudes. In other words, (21) gives the condition that existence of the ith mode with its steady-state amplitude can

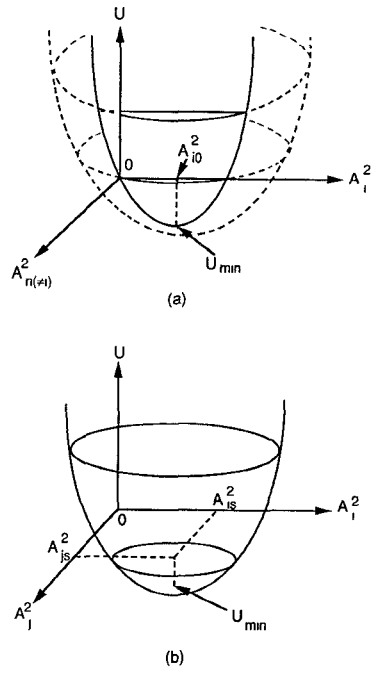

Fig. 5. Topological expression of the averaged potential U. Though U is defined on the multi-dimensional space with A_m^2-axes ($m = 1, 2H, 2L, 3H, \cdots$), U is expressed topologically on the space with only two axes for convenience. Nonnegative region of A_m^2 should be considered. Dotted curves express U in the negative region of A_m^2. (a) In the case when single-mode excitation of the ith mode is stable. (b) In the case when double-mode excitation of the ith and jth mode is stable. U varies along the axes except A_i^2- and A_j^2-axis in a similar manner as along A_n^2-axis in (a).

suppress all other modes. Using (15a) and (17), one can write (21) as

$$\theta_{ii} < \theta_{ni} \quad \text{for all } n\ (\neq i)\,. \tag{22}$$

As for the simultaneous double-mode oscillation of the ith and the jth mode, the steady-state amplitude A_{is} and A_{js} can be obtained from the condition $\partial U/\partial A_i|_{A_i=A_{is},A_j=A_{js},A_{m(\neq i,j)}=0} = 0$ and $\partial U/\partial A_j|_{A_i=A_{is},A_j=A_{js},A_{m(\neq i,j)}=0} = 0$ as

$$A_{is}^2 = (\alpha_i\theta_{jj} - \alpha_j\theta_{ij})/\Theta_{ij} \tag{23a}$$

$$A_{js}^2 = (\alpha_j\theta_{ii} - \alpha_i\theta_{ij})/\Theta_{ij} \tag{23b}$$

(See Fig. 5(b)) where

$$\Theta_{ij} = \begin{vmatrix} \theta_{ii} & \theta_{ij} \\ \theta_{ij} & \theta_{jj} \end{vmatrix}. \tag{23c}$$

The corresponding stability condition is given by the following two inequalities. The first inequality is the condition for U to take the minimum near this steady state with respect to A_i^2 and A_j^2; this results in

$$\Theta_{ij} > 0\,. \tag{24a}$$

Speaking physically, (24a) is the condition for both the ith and the jth mode to exist at the same time. The second inequality is the condition which has a similar meaning as (21), that is,

$$\left.\frac{\partial U}{\partial A_n^2}\right|_{A_i=A_{is},A_j=A_{js},A_{m(\neq i,j)}=0} = \frac{1}{4}\left(-\alpha_n + \theta_{ni}A_{is}^2 + \theta_{nj}A_{js}^2\right) > 0 \quad \text{for all } n\ (\neq i,j) \tag{24b}$$

(See Fig. 5(b)). The meaning of (24b) is similar to (21).

For instance, in the case corresponding to Table I ($N = 4$, $\phi_0 = 2\pi$ and $Q_{ex} = 15$), above stability conditions identify the stable modes as follows:

stable single modes: $i = 1, 3_H$ and 3_L

stable double modes: $(2_H, 4_H)$, $(2_H, 4_L)$, $(2_L, 4_L)$ and $(2_L, 4_H)$.

When Q_{ex} is high, the stability of the mode is identified by the approximation in (16) as

stable single modes: $i = 1, (1 + N/2)_H$ and $(1 + N/2)_L$

stable double modes: $\{m_H, (N + 2 - m)_H\}$, $\{m_H, (N + 2 - m)_L\}$, $\{m_L, (N + 2 - m)_L\}$ and $\{m_L, (N + 2 - m)_H\}$, $m = 2, 3, \cdots, [(N + 1)/2]$, $N \geq 3$.

Under this approximation, no more than two modes oscillate simultaneously. A mode with almost uniform voltage distribution at the active devices tends to be a stable single mode, while a pair of modes which have complementarily nonuniform distributions to each other tend to form a stable double mode.

C. Competitive Growth of Modes

Time evolution of the mode amplitudes and phases can be given by the averaged potential [14] as

$$\frac{dA_i}{dt} = -\frac{1}{I_i}\frac{\partial U}{\partial A_i} = \frac{1}{2I_i}\left(\alpha_i - \theta_{ii}A_i^2 - \sum_{j\neq i}\theta_{ij}A_j^2\right)A_i \tag{25a}$$

$$\frac{d\psi_i}{dt} = 0 \qquad i = 1, 2, \cdots \tag{25b}$$

with

$$I_i = C\left[1 + \frac{1}{Q_{ex}}\frac{2\pi}{\lambda_0}\sum_{k=1}^{N-1}\int_{k\text{th coupling line}}\{p_i(x)\}^2\,dx\right] \tag{25c}$$

where λ_0 is the wavelength on the coupling lines at $\omega = \omega_0$ and $p_i(x)$ is the standing wave voltage distribution on the lines in the ith mode as shown in Fig. 4 (See Appendix II). The voltage distribution $p_i(x)$ on the kth coupling line can be obtained from the voltages at both ends of the kth line, p_{ki} and $p_{k+1,i}$, and the wavelength at the frequency of the ith mode. I_i can be thought to be the inertia of the ith mode oscillation.

Just after the dC power supply for the active devices is turned on, each mode starts to grow competitively from the small initial amplitude which is given by the initial noise voltage distribution. The initial condition decides which one of stable single or double modes remains in the final stage through (25). When every mode amplitude is small, (25a)

gives the growth of A_i as

$$A_i(t) \cong A_i(0)\exp\{\alpha_i^t/(2I_i)\} = A_i(0)\exp\left(\frac{C}{2Q_aI_i}\omega_0 t\right) \tag{26a}$$

where

$$Q_a = \omega_0 C/(G_1 - G_L) \tag{26b}$$

is the active Q of each resonant circuit. This shows that if the ith mode has smaller value of I_i, the mode grows faster.

An example of I_i values for the case of $N = 4$ is also shown in Fig. 4. The power combining mode ($i = 1$) has the smallest I_i value due to small $p_1(x)$, because the maxima of standing wave are located at the antenna elements. On the other hand, other undesired modes have relatively large I_i values. In the example given in Fig. 4, we have $\min_{i(\neq 1)}(I_i/I_1) = 1.7$; this minimum value depends only a little on N and tends to increase with Q_{ex}.

Fig. 6 shows the result of simulation of growth of the modes for the case $N = 5, \phi_0 = 2\pi$ and $Q_{\text{ex}} = 15$ where $\tau = \omega_0 t$ and $\tilde{A}_i = A_i/\sqrt{(G_1 - G_L) \div G_3}$. In (a), though the initial amplitude of mode $i = 1$ is one tenth of those of other modes $\left(\tilde{A}_1(0) = 10^{-3}, \tilde{A}_i(0) = 10^{-2}\ (i \neq 1)\right)$, the mode $i = 1$ grows faster and overcomes the other modes. In (b), however, too much difference between these initial amplitudes makes the mode $i = 1$ ultimately decay. The range of the initial amplitudes for the mode $i = 1$ to survive is shown in Fig. 7, which indicates that the probability of survival of the mode $i = 1$ is considerably higher if the initial amplitudes of all modes are relatively low.

IV. Suppression of Undesired Modes

In order to ensure the oscillation at the power combining mode for the system, it is necessary to suppress all the undesired modes.

A. Introduction of Absorbers.

Let us introduce a resistor R at the midpoint of each coupling line of Fig. 1 as shown in Fig. 8(a). Since the electric current through each R at the ith mode is given approximately from the standing wave voltage as shown in Fig. 4, we can find that R gives power loss to the undesired modes without effect on the desired power-combining mode. In the following, we evaluate the effect of R. In the equivalent circuit representation as shown in Fig. 8(b), we have

$$\begin{bmatrix} I_k \\ I_{k+1} \end{bmatrix} = \begin{bmatrix} Y_{11} & Y_{12} \\ Y_{21} & Y_{22} \end{bmatrix} \begin{bmatrix} V_k \\ V_{k+1} \end{bmatrix} \tag{27}$$

where

$$Y_{11} = Y_{22} = \frac{1}{4}\frac{RY_0}{F}Y_0 + j\left\{-\cot\phi + \operatorname{cosec}\phi\,\frac{\left(RY_0\cos\frac{\phi}{2}\right)^2}{4F}\right\}Y_0$$

$$Y_{12} = Y_{21} = -\frac{1}{4}\frac{RY_0}{F}Y_0 + j\operatorname{cosec}\phi\,\frac{\sin^2\frac{\phi}{2}}{F}Y_0 \tag{28a}$$

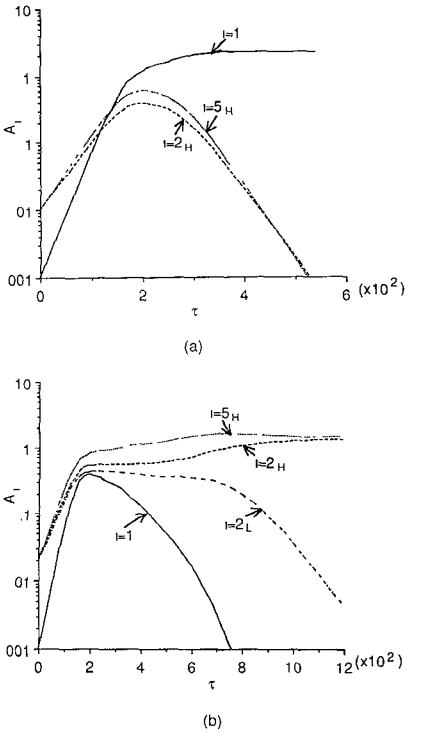

Fig. 6. Simulated result of growth of the modes ($N = 5$, $\phi_0 = 2\pi$, $Q_{\text{ex}} = 15$). Initial condition: (a) $\tilde{A}_1(0) = 10^{-3}$, $\tilde{A}_i(0) = 10^{-2}$ $(i \neq 1)$ (b) $\tilde{A}_1(0) = 10^{-3}$, $\tilde{A}_i(0) = 2 \times 10^{-2}$ $(i \neq 1)$. Amplitudes of typical modes are plotted.

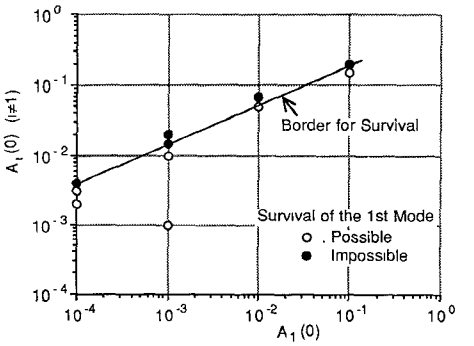

Fig. 7. Initial mode amplitudes for survival of the desired power-combining mode (1st mode).

with

$$F = \sin^2\frac{\phi}{2} + \left(\frac{RY_0}{2}\right)^2\cos^2\frac{\phi}{2}. \tag{28b}$$

The power loss in the kth coupling line is given by

$$\begin{aligned} P_{\text{loss},k} &= (1/2)\,\text{Re}\left(I_kV_k^* + I_{k+1}V_{k+1}^*\right) \\ &= (1/2)\{\text{Re}(Y_{11})\left(|V_k|^2 + |V_{k+1}|^2\right) \\ &\quad + 2\,\text{Re}(Y_{12})\,\text{Re}(V_k^*V_{k+1})\} \end{aligned} \tag{29}$$

where the asterisks denote conjugate quantities.

In case of $RY_0 << 1$, neglecting the change of voltage distribution due to introduction of R, the power loss in the

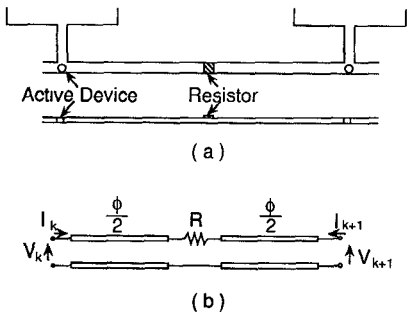

Fig. 8. Introduction of a resistive absorber. (a) A resistor R at the midpoint of each coupling line. (b) Equivalent representation.

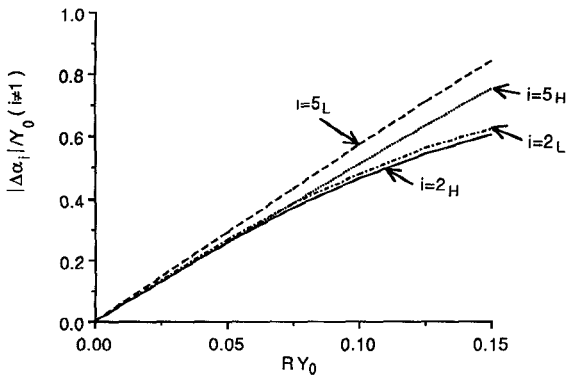

Fig. 9. Dependence of $|\Delta\alpha_i|/Y_0$ $(i \neq 1)$ on RY_0 for the case of $N = 5$, $\phi_0 = 2\pi$, $Q_{ex} = 15$. Results for typical modes are plotted.

kth coupling line is expressed using (13), (28), and (29) as

$$P_{\text{loss},k} = \frac{1}{2}\sum_i A_i^2 \,\text{Re}(Y_{11})(p_{ki} - p_{k+1,i})^2 \qquad k = 1, 2, \cdots, N-1. \tag{30}$$

The increment of the averaged potential due to introduction of all the resistances, ΔU, is given by $(1/2)\sum_{k=1}^{N-1} P_{\text{loss},k}$, which together with (7), (28) and (30) yields

$$\Delta U = -\sum_i \Delta\alpha_i A_i^2 \tag{31a}$$

where

$$\Delta\alpha_i = \begin{cases} 0, & i = 1 \\ -Y_0 \frac{RY_0}{F} \sin^2\frac{\xi_i}{2} \frac{(N-1)\sin\xi_i \mp \sin\{(N-1)\xi_i\}}{N\sin\xi_i \pm \sin(N\xi_i)}, & i \neq 1 \end{cases} \tag{31b}$$

and, hence it is confirmed that the mode $i = 1$ is not affected. In (31b), the upper and the lower sign for $i \neq 1$ correspond to the cos-mode and to the sin-mode, respectively. $|\Delta\alpha_i|$ is the amount of decrease of the gain parameter of the ith mode due to R's. Fig. 9 shows the dependence of $|\Delta\alpha_i|/Y_0$ $(i \neq 1)$ on RY_0 for the case of $N = 5$, $\phi_0 = 2\pi$ and $Q_{ex} = 15$. $|\Delta\alpha_i|(i \neq 1)$ is the smallest for the mode 2_H. The dependence of $|\Delta\alpha_i|$ for the mode 2_H on N is given in Fig. 10; $\min_{i(\neq 1)} |\Delta\alpha_i|$ decreases with increasing N and decreasing Q_{ex}.

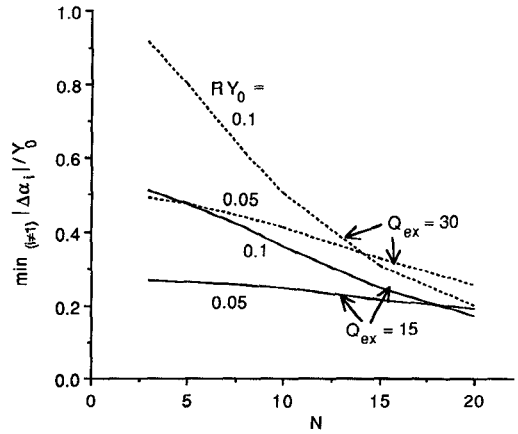

Fig. 10. Dependence of $\min_{i(\neq 1)} \{|\Delta\alpha_i|/Y_0\}$ on N.

B. Suppression of Undesired Modes

Undesired modes can be made unstable when their stability conditions (21) and (24b) with $n = 1$ are no longer satisfied by introduction of R's. Because α_i should be replace by $\alpha_i + \Delta\alpha_i$, such conditions for suppression of undesired modes are written as

$$\alpha_1 - \frac{\theta_{1i}}{\theta_{ii}}(\alpha_i + \Delta\alpha_i) > 0 \qquad \text{for all } i\ (\neq 1) \tag{32a}$$

and for all pairs (i, j) which satisfies (24a),

$$\alpha_1 - \theta_{i1}A_{is}'^2 - \theta_{j1}A_{js}'^2 > 0 \tag{32b}$$

where A_{is}' and A_{js}' are the mode amplitudes obtained by (23) with above replacement for α_i and α_j. These inequalities mean that the desired 1st mode can grow even if there exists an undesired single-mode or an undesired double-mode oscillation with the steady-state mode amplitude.

In the case of a high Q_{ex}, using (16) in (32a) gives

$$|\Delta\alpha_i| > \begin{cases} \frac{1}{4}(G_1 - G_L) & \text{for } i \neq 1 + N/2 \\ \frac{1}{2}(G_1 - G_L) & \text{for } i = 1 + N/2. \end{cases} \tag{33}$$

For (32b), the sufficient condition is written as

$$\min_{i(\neq 1)}(|\Delta\alpha_i|) > \frac{3}{8}(G_1 - G_L) \tag{34}$$

Summing (33) and (34), we obtain the sufficient condition for suppressing all the undesired modes as

$$\min_{i(\neq 1)}(|\Delta\alpha_i|) > \begin{cases} \frac{1}{2}(G_1 - G_L) & \text{for even } N \\ \frac{3}{8}(G_1 - G_L) & \text{for odd } N. \end{cases} \tag{35}$$

When the load conductance G_L is optimized for maximum output power, the term $G_1 - G_L$ in above inequalities becomes $G_1/2$.

V. Experiment

Experiment was carried out for the arrays with two, four and eight oscillator units using packaged Gunn diodes manufactured by Alpha Industries.

Large-signal admittance of each Gunn diode was measured at the design frequency 12.45 GHz. A single microstrip Gunn

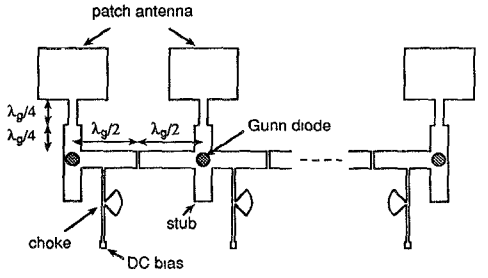

Fig. 11. Configuration of the oscillator array.

diode oscillator was constructed, and the maximum output power at the design frequency was obtained by adjusting the load admittance. The averaged maximum output power and the corresponding load admittance Y_L were 4.0 mW (6.0 dBm) and $12.7-j14.1$ mS, respectively. The large-signal Gunn diode admittance is then given as $-Y_L$ [6].

The oscillator arrays were fabricated as shown in Fig. 11 using Duroid 5870 with a thickness of 31 mil and a relative dielectric constant of 2.33. Each patch antenna oscillator unit was designed by use of CAD so that it can oscillate at 12.45 GHz and can generate the maximum output power. Note that these units are not yet connected together as the gaps are provided between adjacent units. A two-stage quarter wavelength transformer between the patch antenna and the diode was used for admittance matching. An open stub was attached to each Gunn diode for fine tuning. All the Gunn diodes had common DC bias voltage. However, there were still small variations in the characteristics of the oscillator units. In the case of the array with eight units, for instance, the free-running oscillation frequency and the effective radiation power (ERP) of each unit were on the average 12.452 GHz and 13.2 dBm with the maximum deviation of 15 MHz and 1.4 dBm, respectively.

First, adjacent units were connected with a conductor strip with its width almost identical to that of the coupling microstrip lines. In this case, though a single frequency spectrum of the in-phase mode was observed for the two unit array, oscillation with a single frequency spectrum could not be obtained for the four-unit and the eight-unit arrays. Fig. 12(a) shows the spectrum of the output received in the broadside direction of the eight unit array. Similar spectrum was observed for the four-unit array. Measurement of the directivity pattern of each frequency showed that different frequencies with different patterns were contained. It is conjectured from this spectrum that either of the following two types of oscillations was excited in the four-unit and the eight-unit arrays. One type is the simultaneous multi-mode oscillation with interactions between the constituent modes. The other type is the unlocked oscillation in which the active antennas in the major part of the array are locked together, while the remainders are unlocked. This is strictly a conjecture and requires a further study.

Next, a chip resistor was introduced between adjacent oscillator units in order that only the in-phase power-combining mode can oscillate. Resistors of 2 Ω were not sufficient to stabilize the in-phase mode for the four-unit and the eight-unit arrays. When chip resistors of 4.7 Ω were used, stable

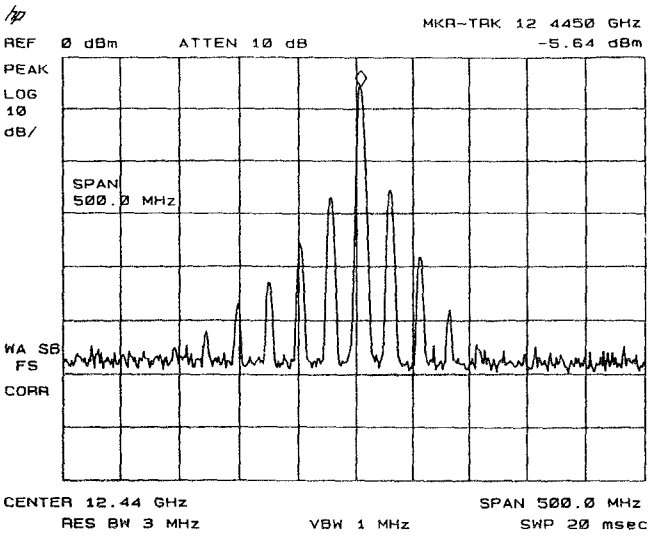

(a)

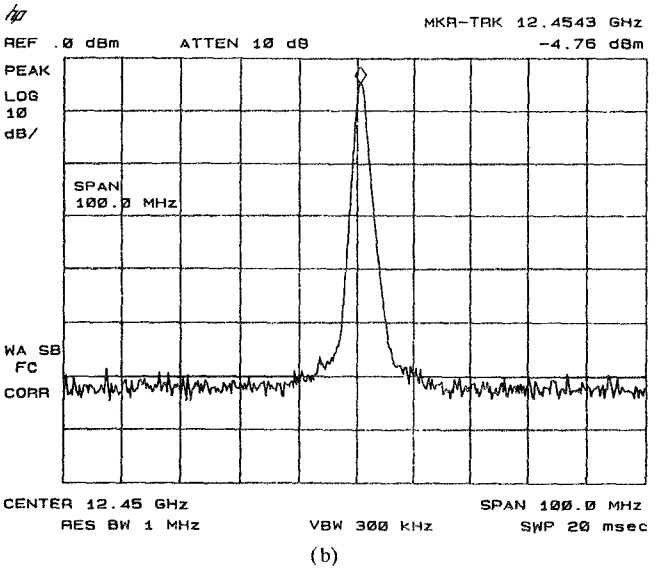

(b)

Fig. 12. Spectrum of the 8-unit oscillator array. (a) In the case of direct connection between adjacent oscillator units. (b) In the case of connecting adjacent oscillator units with 4.7 Ω resistors.

oscillation of the in-phase mode was easily obtained for all the cases of two-unit, four-unit and eight-unit arrays. For the eight unit array, the spectrum is shown in Fig. 12(b), while the H-plane and E-plane radiation pattern are shown in Fig. 13 with comparison of theoretical values. The cross polarization ratio was larger than 25 dB. The ERP's of two-unit, four-unit and eight-unit arrays were 19.1 dBm, 25.1 dBm, and 30.4 dBm, respectively. The increment of about 6 dB shows that stable power combining with very high efficiencies can be attained.

The suitable value of the resistance to suppress the undesired modes was determined by equation (35) and Fig. 9. From (35), the smallest value of $|\Delta\alpha_i|$ must be larger than $(G_1 - G_L)/2$. Since the oscillator was designed by maximizing the output power at 12.45 GHz, the load admittance Y_L was equal to the negative value of the device admittance Y_D. As described above, Y_L was equal to $12.7-j14.1$ mS. Therefore, G_L was equal to 12.7 mS. From (20), G_L was equal to $G_1/2$ for

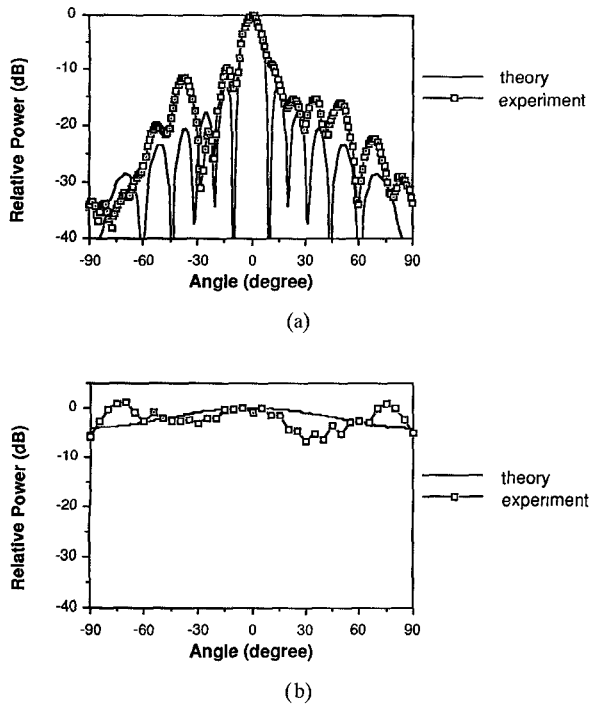

Fig. 13. Radiation patterns of the array with eight oscillator units (a) H-plane pattern (b) E-plane pattern.

the nonlinear device model in (11). With these information, $(G_1 - G_L)/2 = G_L/2 = 6.35$ mS was calculated. Normalized by the characteristic admittance of the coupling line Y_0, the smallest value of $|\Delta\alpha_i|/Y_0$ must be larger than 0.3175 for the suppression of all the undesired modes. From Fig. 9, it can be reasonably stated that $RY_0 = 0.07$ was sufficient to suppress all the undesired modes. Therefore, the sufficient value of R was 3.5 Ω. The above calculation is based on the approximation of $Q_{\text{ex}} \cong 15$. Considering the possible errors of the data used in calculation, we selected a larger value of 4.7 Ω. The experimental result shows that the resistors of 4.7 Ω were able to stabilize the in-phase mode oscillation while the resistors of 2 Ω were not.

The oscillator arrays in the experiment had some complicated factors which cannot be considered in the theory: unevenness of the free-running oscillation frequency and the output power of each unit, the narrow bandwidth of the patch antennas and the complex characteristics of Gunn diodes. Therefore, it is not easy to explain the experimental results in detail using the mode theory. However, it can be concluded that the theory is effective in letting only the in-phase mode oscillate by the proposed insertion of resistors.

VI. Conclusion

For a one-dimensional array of active microstrip antennas with strongly coupled oscillators, a mode analysis of the array has been presented, and an effective method for obtaining a stable in-phase power-combining operation has been proposed.

In the mode analysis, the frequencies and the voltage distributions of the normal modes of the array have been obtained. Stable modes of the array have been identified using the averaged potential on the assumption that the active devices have cubic voltage-current characteristics. Simulation of time evolutions of the mode amplitudes have indicated that the probability of survival of the in-phase power-combining mode is high if the initial amplitudes of all modes are relatively low. It has been shown analytically that only the oscillation of the in-phase power-combining mode can be excited when appropriate resistors are introduced at the midpoints of the coupling lines between the oscillators.

An experiment for two-unit, four unit, and eight-unit array using Gunn diodes has confirmed that the introduction of appropriate resistors is effective in exciting only the in-phase power-combining mode. In contrast, when each oscillator unit was connected directly using conductors, a single spectrum could not be obtained in the arrays with more than four units; the oscillation spectra are not easily explained by the mode theory.

The mode theory presented here has treated an idealized active antenna array. The theory has assumed that all the units of the array are identical and the active devices have cubic voltage-current characteristics. It is planned to improve the theory so as to be able to treat actual arrays with variations of the elements.

It is important to investigate the behavior of the active antenna array when some active devices fall into trouble. It is also significant to attain stable in-phase power-combining operation in a two-dimensional array with a very large number of active microstrip antennas. These are left for future study.

Appendix I

For the ith eigenvalue λ_i and eigenvector $\boldsymbol{P}_i = [p_{1i}, p_{2i}, \cdots, p_{Ni}]^t$ of the matrix $\boldsymbol{B}$, the equation $[\boldsymbol{B} - \lambda_i \boldsymbol{E}]\boldsymbol{P}_i = 0$, where $\boldsymbol{E}$ is a unit matrix, together with (4a) gives

$$p_{k-1,i} + (2\gamma - \lambda_i)p_{ki} + p_{k+1,i} = 0, \qquad k = 2, 3, \cdots, N-1 \tag{A1}$$

with the boundary condition

$$(\gamma - \lambda_i)p_{1i} + p_{2i} = 0 \tag{A2a}$$

$$p_{N-1,i} + (\gamma - \lambda_i)p_{Ni} = 0\,. \tag{A2b}$$

Assuming the variation of p_{ki} as $e^{\beta_i k}$ because of structural periodicity, (A1) yields

$$e^{2\beta_i} + (2\gamma - \lambda_i)e^{\beta_i} + 1 = 0\,. \tag{A3}$$

We can represent two roots for e^{β_i} as $e^{j\xi_i}$ and $e^{-j\xi_i}$, since (A3) shows the product of the two roots equals to unity. Equation (6a) can be obtained using (A3).

The general expression for p_k can be given as

$$p_{ki} = C_1 e^{j(k-1)\xi_i} + C_2 e^{-j(k-1)\xi_i}\,. \tag{A4}$$

Substituting (A4) and (6a) into (A2) gives

$$\begin{bmatrix} \gamma + e^{-j\xi_i} & \gamma + e^{j\xi_i} \\ (\gamma + e^{j\xi_i})e^{j(N-1)\xi_i} & (\gamma + e^{-j\xi_i})e^{-j(N-1)\xi_i} \end{bmatrix} \begin{bmatrix} C_1 \\ C_2 \end{bmatrix} = \begin{bmatrix} 0 \\ 0 \end{bmatrix}. \tag{A5}$$

In order for C_1 and C_2 to have nontrivial solutions, the determinant of the matrix in the left hand side of (A5) should

vanish, which yields (6b). Substituting the ratio C_1/C_2 into (A4) gives (7) as a normalized expression.

APPENDIX II

M. Kuramitsu and F. Takase originally developed the averaged potential theory for lumped-element circuit systems [14]. In order to apply this theory to the circuit with transmission lines in Fig. 2, we represent TEM transmission lines equivalently as conventional ladder networks with series inductances $l_0\Delta x$'s and shunt capacitances $c_0\Delta x$'s, where Δx is the length of each infinitesimal section of the lines, and c_0 and l_0 are the capacitance and the inductance for the line of unit length, respectively.

For the equivalent circuit, the time variation of mode amplitudes can be given by (25a) with

$$I_i = \sum_m c_m p_{mi}^2 \tag{A6}$$

where the summation is taken over all the capacitances, and p_{mi} is the voltage distribution of the ith mode at the mth capacitance. Equation (A6) is written as

$$I_i = C\sum_{k=1}^{N} p_{ki}^2 + c_0 \int_{\text{coupling lines}} \{p_i(x)\}^2\, dx \tag{A7}$$

which gives (25c) using the relations $Y_0 = \sqrt{c_0/l_0}$, $1/\sqrt{c_0 l_0} = \omega_0\lambda_0/(2\pi)$ and (2g).

ACKNOWLEDGMENT

The authors would like to thank Dr. T. Hirota and Mr. S. Kawasaki for their valuable advice in the experiment. This work was supported by the U.S. Army Research Office under contract DAAL 03-88-K-0005.

REFERENCES

[1] K. Chang and C. Sun, "Millimeter-wave power combining techniques," *IEEE Trans. Microwave Theory Tech.*, vol. MTT-31, pp. 91–107, Feb. 1983.
[2] J. W. Mink, "Quasi-optical power combining of solid-state millimeter-wave sources," *IEEE Trans. Microwave Theory Tech.*, vol. MTT-34, pp. 273–279, Feb. 1986.
[3] Z. B. Popovic, R. M. Weikle II, M. Kim, and D. B. Rutledge, "A 100-MESFET planar grid oscillator," *IEEE Trans. Microwave Theory Tech.*, vol. 39, pp. 193–200, Feb. 1991.
[4] H. Kondo, M. Hieda, M. Nakayama, T. Tanaka, K. Osakabe, and K. Mizuno, "Millimeter and submillimeter wave quasi-optical oscillator with multi-elements," *IEEE Trans. Microwave Theory Tech.*, vol. 40, pp. 857–863, May 1992.
[5] R. A. York and R. C. Compton, "Quasi-optical power combining using mutually synchronized oscillator arrays," *IEEE Trans. Microwave Theory Tech.*, vol. 39, pp. 1000–1009, June 1991.
[6] A. Mortazawi, H. D. Foltz, and T. Itoh, "A periodic second harmonic spatial power combining oscillator," *IEEE Trans. Microwave Theory Tech.*, vol. 40, pp. 851–856, May 1992.
[7] S. Kawasaki and T. Itoh, "40 GHz quasi-optical second harmonic spatial power combining using FETs and slots," in *1992 IEEE MTT-S Int. Microwave Symp. Dig.*, June 1992, pp. 1543–1546.
[8] J. Birkeland and T. Itoh, "Two-port FET oscillators with applications to active arrays," *IEEE Microwave Guided Wave Lett.*, vol. 1, pp. 112–113, May 1991.
[9] ——, "A 16 element quasi-optical FET oscillator power combining array with external injection locking," *IEEE Trans. Microwave Theory Tech.*, vol. 40, pp. 475–481, Mar. 1992.
[10] K. Chang, K. A. Hummer, and J. L. Klein, "Experiments on injection locking of active antenna elements for active phased arrays and spatial power combiners," *IEEE Trans. Microwave Theory Tech.*, vol. 37, pp. 1078–1084, July 1989.
[11] S. Nogi and K. Fukui, "Optimum design and performance of a microwave ladder oscillator with many diode mount pairs," *IEEE Trans. Microwave Theory Tech.*, vol. MTT-30, pp. 735–743, May 1982.
[12] K. Fukui and S. Nogi, "Mode analytical study of cylindrical cavity power combiners," *IEEE Trans. Microwave Theory Tech.*, vol. MTT-34, pp. 943–951, Sept. 1986.
[13] K. D. Stephan and S. L. Young, "Mode stability of radiation-coupled interinjection-locked oscillators for integrated phased arrays," *IEEE Trans. Microwave Theory Tech.*, vol. 36, pp. 921–924, May 1988.
[14] M. Kuramitsu and F. Takase, "Analytical method for multimode oscillators using the averaged potential," *Elec. Commun. Japan*, vol. 66-A, pp. 10–19, 1983.

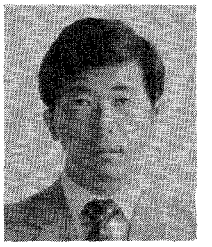

Shigeji Nogi (M'88) was born in Osaka prefecture, Japan, on December 26, 1945. He received the B.E., the M.E., and the D.Eng. degrees in electronic engineering from Kyoto University, Kyoto, Japan, in 1968, 1970, and 1984, respectively.

From 1970 to 1972, he was employed by the Central Research Laboratory, Mitsubishi Electric Corporation, Amagasaki, Japan. In 1972 he joined the Department of Electronics, Okayama University, Okayama, Japan, where he is now an Associate Professor. In the 1991–92 academic year, he spent a ten-month sabbatical leave at the University of California, Los Angeles. He has been engaged in research on microwave active circuits, multimode oscillators, and nonlinear wave propagation.

Dr. Nogi is a member of the Institute of Electronics, Information and Communication Engineers of Japan and the Institute of Television Engineers of Japan.

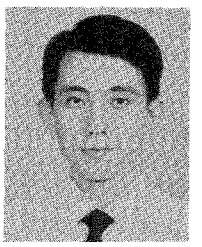

Jenshan Lin (S'91) was born in Keelung, Taiwan on December 11, 1964. He received the B.S. degree in Electrophysics from the National Chiao Tung University, Hsinchu, Taiwan, in 1987 and the M.S. degree in Electrical Engineering from the University of California, Los Angeles, in 1991.

From 1989 to 1990 he was with the Center for Measurement Standards, Industrial Technology Research Institute, Hsinchu, Taiwan. Since 1991 he has been a Graduate Student Researcher in the Microwave and Millimeter Wave Electronics Laboratory in UCLA, where he is currently working toward the Ph.D. degree. His research interests include microwave active circuits and active antenna arrays.

Tatsuo Itoh (S'69–M'69–SM'74–F'92) received the Ph.D. Degree in Electrical Engineering from the University of Illinois, Urbana in 1969.

From September 1966 to April 1976, he was with the Electrical Engineering Department, University of Illinois. From April 1976 to August 1977, he was a Senior Research Engineer in the Radio Physics Laboratory, SRI International, Menlo Park, CA. From August 1977 to June 1978, he was an Associate Professor at the University of Kentucky, Lexington. In July 1978, he joined the faculty at the University of Texas at Austin, where he became a Professor of Electrical Engineering in 1981 and Director of the Electrical Engineering Research Laboratory in 1984. During the summer of 1979, he was a guest researcher at AEG-Telefunken, Ulm, West Germany. In September 1983, he was selected to hold the Hayden Head Centennial Professorship of Engineering at The University of Texas. In September 1984, he was appointed Associate Chairman for Research and Planning of the Electrical and Computer Engineering Department at The University of Texas. In January 1991, he joined the University of California, Los Angeles as Professor of Electrical Engineering and holder of the TRW Endowed Chair in Microwave and Millimeter Wave Electronics.

Dr. Itoh is a member of the Institute of Electronics and Communication Engineers of Japan, Sigma Xi, and Commissions B and D of USNC/URSI. He served as the Editor of IEEE TRANSACTIONS ON MICROWAVE THEORY AND TECHNIQUES for 1983–1985. He serves on the Administrative Committee of IEEE Microwave Theory and Techniques Society. He was Vice President of the Microwave Theory and Techniques Society in 1989 and President in 1990. He is the Editor-in-Chief of *IEEE Microwave and Guided Wave Letters*. He was the Chairman of USNC/URSI Commission D from 1988 to 1990 and is the Vice Chairman of Commission D of the International URSI.